PWR LATTICE BENCHMARK PROBLEMS

Joint Benchmark Committee
of the
Mathematics and Computation, Radiation Shielding and Protection, and
Reactor Physics Divisions of the American Nuclear Society

Initially developed and distributed by:
Ad Hoc Committee on Reactor Physics Benchmarks
Reactor Physics Division
American Nuclear Society

Table of Contents

1. INTRODUCTION

Many benchmark activities which are mathematical in nature provide an excellent means to compare and validate various calculational methods and codes. In these benchmarks, the material properties, including nuclear cross sections, are specified. Therefore, these problems cannot address the nuclear data and cross section processing methodology and codes.

The only manner in which nuclear data can be validated is by the comparison of calculated values with experimental measurements. The benchmark problems presented herein are based upon clean light water reactor (LWR) assembly experiments performed by Babcock and Wilcox (B&W) in the early 1970s. Three assembly configurations are given which have a progression in heterogeneity from an assembly with only fuel pins (assembly type A), to an assembly with fuel pins and water holes (assembly type B), to an assembly with fuel pins, water holes, and perturbing (absorber) pins (assembly type C). The experimental measurements were of critical boron concentrations and rod-by-rod fission distributions. More information on the experimental configuration is provided in Section 2, and the benchmark specifications are given in Section 3.

These problems are well suited for analysis by assembly codes as well as Monte Carlo codes. Calculations of the critical core configurations can be compared directly to the measurements in order to assess the accuracy of the cross section data and processing methodology. Additional calculated parameters for each assembly type may prove useful in a comparison of different nuclear data and methodologies. Note that, as presented, these benchmark problems are intended for 2-dimensional analysis, although sufficient information is given for 3-dimensional analysis. A description of the desired results is given in Section 4.

The primary goal of this benchmark is to provide an inter-comparison of nuclear data and related processing codes. The exchange of information will provide substantial information for determining the strengths and weaknesses of the various approaches for LWR analysis.

The benchmark experiments are documented in Ref. 1. The specifications for this benchmark were adapted from Ref. 2. A special session at the 1998 *International Conference on the Physics of Nuclear Science and Technology* was devoted to this benchmark and the submitted solutions, and the interested reader is referred to the summary paper (Ref. 3) and other papers in that session.

2. OVERVIEW OF THE EXPERIMENTS

Beginning in January 1970, a series of experiments with heterogeneous lattices of low-enriched UO_2 fuel pins was performed at B&W's Lynchburg Research Center. The research was supported jointly by B&W and the U. S. Atomic Energy Commission and was completed in 1971. The experiments were performed inside a large aluminum tank containing borated water, UO_2 fuel pins, and a number of so-called perturbing pins. The fuel pins contained low-enriched uranium (LEU) and were clad in aluminum. The water contained soluble boron in the form of dissolved boric acid (H_3BO_3). The water height was exactly 145 cm, and the boron concentration in the water was adjusted until each experimental configuration was slightly supercritical, with a value of 1.0007 for k_{eff}. The soluble boron concentration for each experiment was determined by titration and reported in units of parts per million by weight (ppm) in water. The standard deviation for each soluble boron concentration is ± 3 ppm.

For most of these experiments, the central region of the core closely resembled a 3x3 array of pressurized water reactor (PWR) fuel assemblies with fuel pins arranged in a 15x15 lattice. The nine assemblies were surrounded by a driver region of LEU fuel pins identical to those in the assemblies. The driver region had an irregular outer boundary, as shown in Figure 2.1. The region between the driver boundary and the inner wall of the tank contained only water. The vertical dimensions of the core are shown in Fig. 2.2. This figure shows the 2-inch-thick aluminum base plate located one inch above the bottom of the tank. Also shown are the upper and lower grids, which consist of 1-inch-wide slotted aluminum strips interlocked to form a square matrix.

Sixteen different configurations or, in B&W's terminology, "loadings" were considered for this particular core configuration (core XI), with each loading differing in the number of water holes and perturbing pins. Loadings 1, 2, and 8 were selected for use in this benchmark and have been designated as assembly types A, B, and C, respectively.

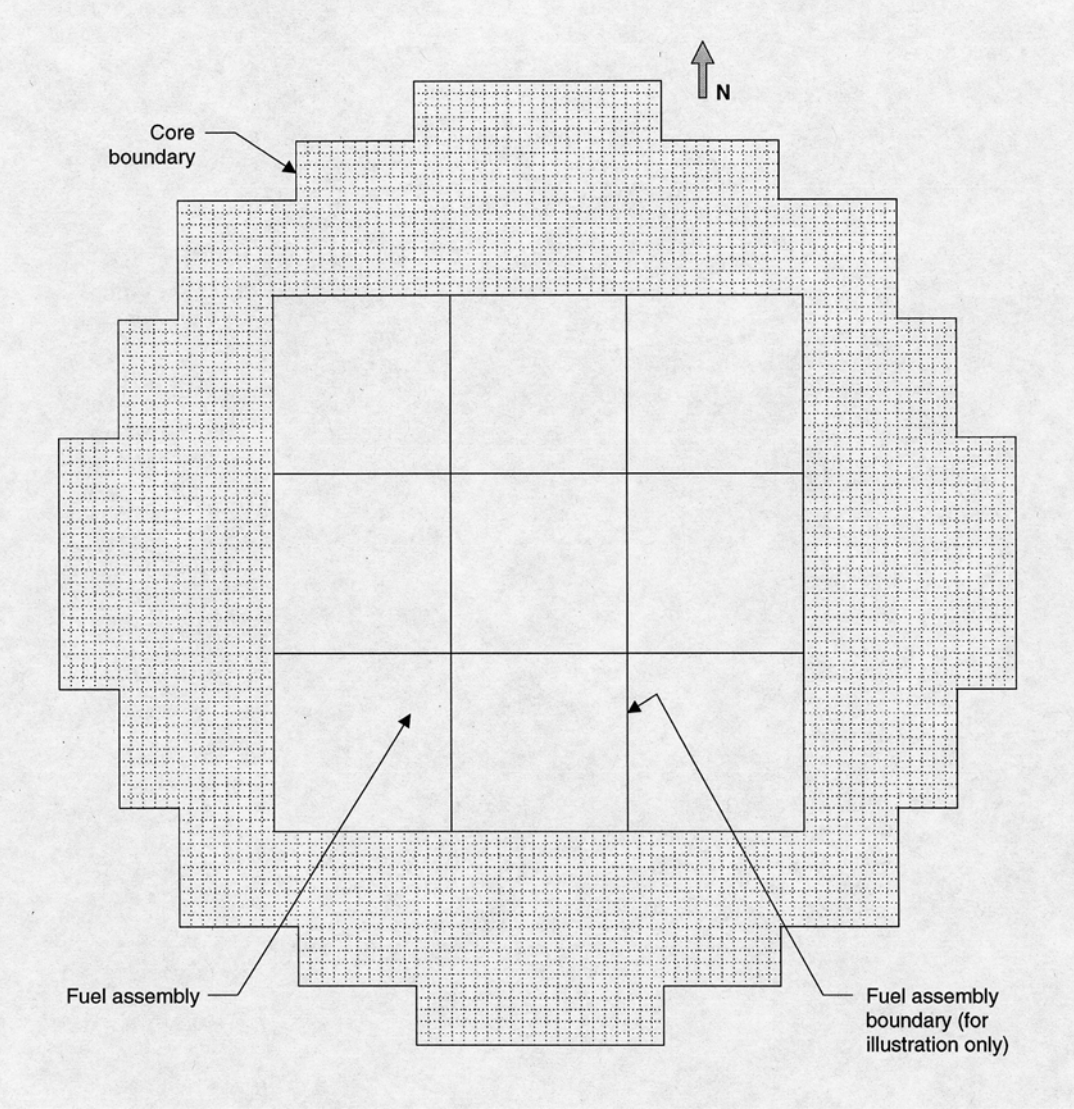

Fig. 2.1 Core Diagram (taken directly from Ref. 1).

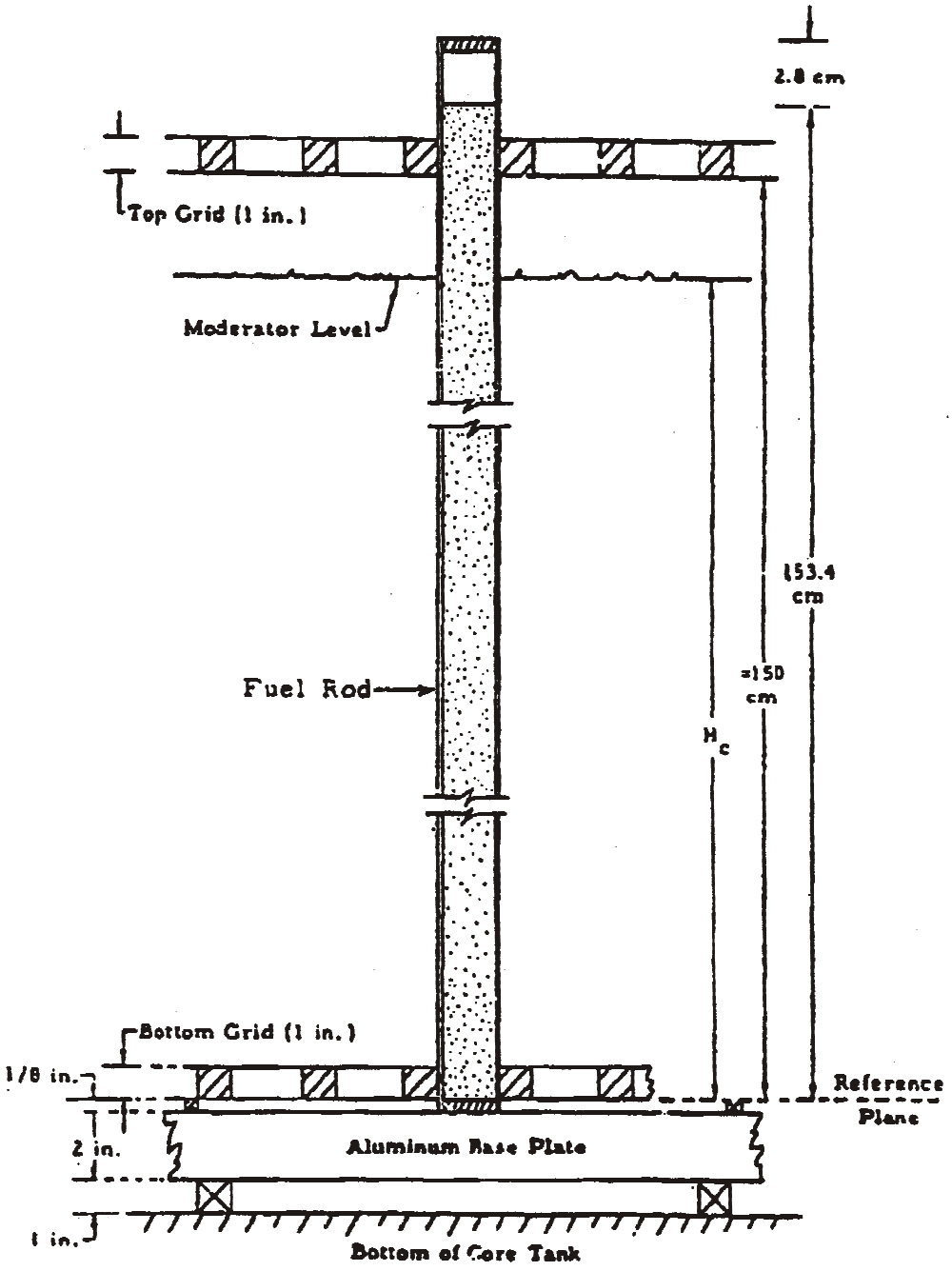

Fig. 2.2 Vertical core dimensions (taken directly from Ref. 1).

3. BENCHMARK SPECIFICATIONS

3.1 Core Description

The core configuration is shown in Fig. 2.1 and consists of a 3x3 array of PWR fuel assemblies surrounded by a driver region. The driver region contains LEU fuel rods identical to those used in the central nine assemblies. The central nine assemblies are varied for the three different benchmark problems. The region between the driver region and the inner wall of the tank contains only borated water. The outer radius of the water reflector is 30 inches (76.20000 cm). The aluminum tank is 0.5-in (1.27000 cm) thick but can be omitted from the benchmark models because it does not significantly affect the core reactivity.

3.2 Assembly Description

The assemblies consist of a 15x15 array of fuel pins, water holes, and perturbing pins. All of the loadings are laid out on a square pitch of 0.644 inches (1.63576 cm). It should be noted that the water holes contain only water; i.e., no structural elements such as guide tubes are present.

Assembly type A contains fuel rods in all locations and, therefore, is indistinguishable from the driver region.

Assembly type B contains 17 water holes arranged in the same configuration as a standard 15.x15 fuel assembly for a commercial PWR. The locations of the water holes are shown in Fig. 3.1.

Assembly type C is identical to type B except that Pyrex rods have been inserted into all of the water holes except the central hole. The layout of assembly type C is shown in Fig. 3.2.

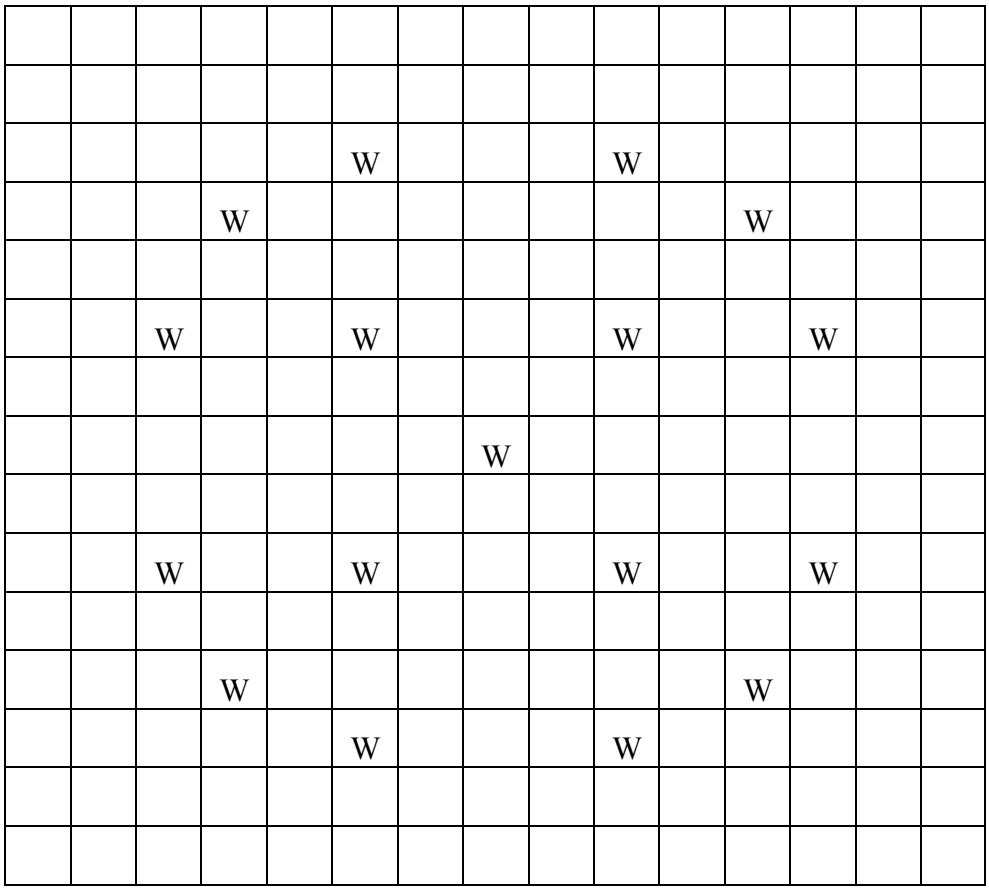

W = Water Hole

Fig. 3.1 Assembly type B.

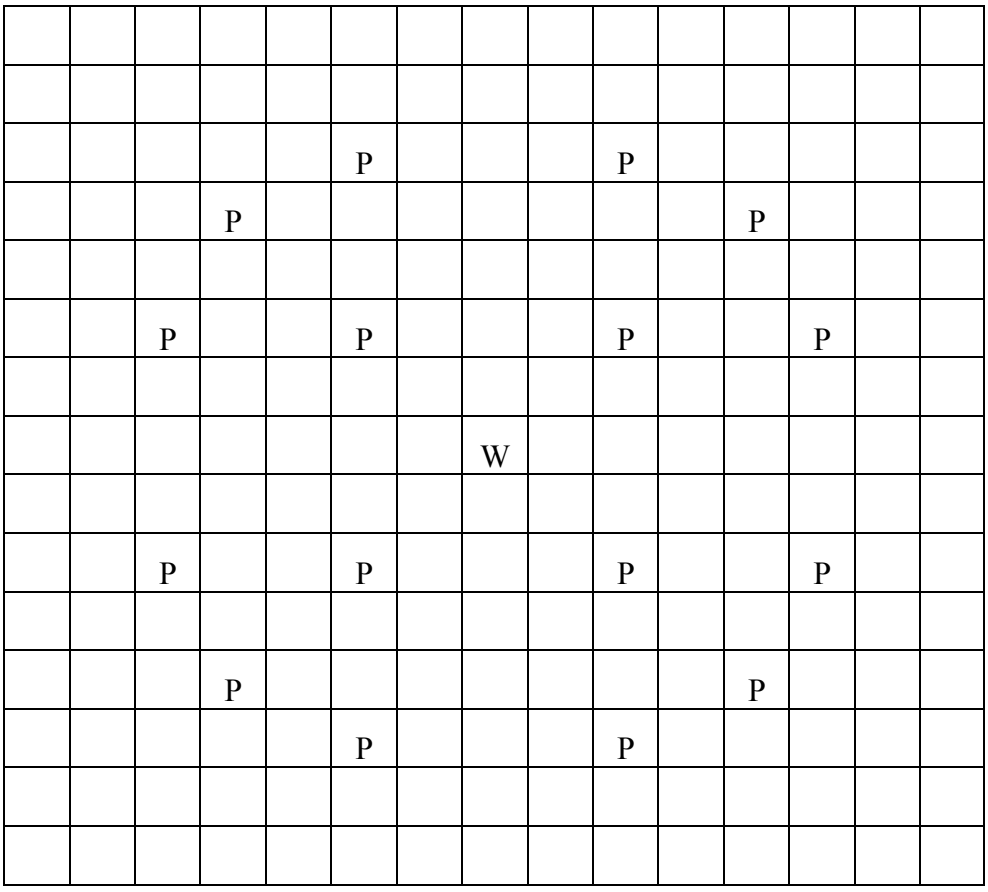

P = Pyrex Rod W = Water Hole

Fig. 3.2 Assembly type C.

3.3 Fuel Pins

The principal physical description of the fuel pins is given in Table 3.1. Reference 1 states that the fuel pellets contain a low level of impurities which is characterized by a macroscopic absorption cross section that is less than 0.001 cm^{-1} at 2200 m/s. These impurities can be modeled by inserting a concentration of boron that produces an increment of 0.001 cm^{-1} in the macroscopic absorption cross section of the fuel at 2200 m/s. As Table 3.1 shows, the ^{235}U enrichment is 2.459 wt.%. Assume that the concentration of ^{234}U (in wt.%) is 0.008 times the enrichment (0.019672 wt.%) and that the remainder is ^{238}U (97.521 wt.%). The cladding of the fuel rods is a tube of aluminum 6061, for which the specifications are given in Table 3.2. A standard composition for aluminum 6061 is given in Table 3.3.

Table 3.1 Characteristics of UO_2 fuel pins.

Parameter	Value	
	Reported	**Benchmark**
Pellet Diameter	0.4054 ± 0.0005 in	1.029716 cm
Active Length	60.37 ± 0.35 in	153.3398 cm
Mass per Fuel Pin	1305.5 ± 1.0 g	1305.5000 g
Pellet Density	10.24 ± 0.04 g/cm^3	10.2400 g/cm^3
Enrichment (wt.%)	2.459 ± 0.002 wt.%	2.4590 wt.%
^{235}U Mass	28.29 ± 0.02 g	28.2900 g

Table 3.2 Characteristics of fuel pin cladding.

Parameter	Value	
	Reported	**Benchmark**
Material	Al-6061	Al-6061
Density	(not reported)	2.7000 g/cm^3
Outer Diameter	0.4748 ± 0.00006 in	1.205992 cm
Thickness	0.032 ± 0.001 in	0.081280 cm
Length	61.59 ± 0.16 in	156.4386 cm

Table 3.3 Composition for aluminum-6061 (from Ref. 4).

Element	Composition (wt.%)
Mg	1.00
Al	96.55
Si	0.60
Ti	0.15
Cr	0.20
Mn	0.15
Fe	0.70
Cu	0.25
Zn	0.25
Others	0.15

3.4 Perturbing Pins

Assembly type C contains Pyrex perturbing pins. The characteristics of the perturbing pins are given in Table 3.4. The Pyrex contains 12.615 wt.% of boron oxide (B_2O_3), 4 wt.% Na_2O, and 2 wt.% aluminum (Refs. 1 and 5). The remainder of the Pyrex (81.385 wt.%) is SiO_2. The boron oxide content corresponds to 3.919 wt.% natural boron, and it is assumed that natural boron contains 18.43 wt.% ^{10}B. These perturbing pins do not have a cladding.

Table 3.4 Characteristics of perturbing pins.

Parameter	Value	
	Reported	**Benchmark**
Diameter	1.170 ± 0.001 cm	1.1700 cm
Length	188.0 ± 0.1 cm	188.0000 cm
Mass	453.6 ± 0.6 g	453.6000 g
Density	(not reported)	2.24416 g/cm^3

3.5 Water and Soluble Boron

The temperature of the water is taken to be 20° C (see Section 3.6), resulting in a density of 0.99823 g/cm^3 (Ref. 5). The boron concentrations are given in Table 3.5 for the critical core configurations with assembly types A, B, and C.

3.6 Temperatures

Since the experiments were performed under standard laboratory conditions, a temperature of 20° C is assumed.

3.7 Axial Buckling

The axial buckling of the core configuration was experimentally determined and can be used as input for 2-dimensional modeling. The axial buckling is 0.00037 cm^{-2} (Ref. 2), which corresponds to an axially uniform model with a height of 163.324 cm.

Table 3.5 Boron concentrations in water.

	Critical Soluble Boron Concentration (ppm)		Critical Soluble ^{10}B Concentration (ppm)[a]
Assembly Type	**Reported**	**Benchmark**	**Benchmark**
A (Loading 1)	1511 ± 3	1511	278.5
B (Loading 2)	1335.5 ± 3	1335.5	246.1
C (Loading 8)	794 ± 3	794	146.3

[a]Assumes that natural boron contains 18.43 wt.% ^{10}B

4. MODELING INSTRUCTIONS AND DESIRED RESULTS

The benchmark problems are to be modeled using the specifications presented in Section 3. In addition to a comparison of calculated quantities with measured quantities, a number of calculated parameters have been proposed for which there are no measured results. Note that the calculation of the isotopic number densities is considered to be part of the analysis, and they are to be included in the submission of results to facilitate the comparison of results.

4.1 Core Calculations

A comparison against the measured quantities requires a 2-dimensional analysis (with the buckling supplied) or a 3-dimensional analysis of the core. Note, however, that these benchmark problems are intended primarily for 2-dimensional analysis. This involves the modeling of the central nine assemblies, the driver region, and the water reflector. The benchmark problems have symmetry such that eighth-core or quarter-core models may be used.

The benchmark multiplication factor for all three problems is 1.0007 ± 0.0008. The only two significant contributors to the uncertainty in reactivity are the uncertainties in the soluble boron concentration and the axial buckling. Calculations with the MCNP4C2 Monte Carlo code (Ref. 6) and nuclear data derived from Release 4 of ENDF/B-VI indicate that the uncertainty in k_{eff} corresponding to the reported uncertainty of ±3 ppm in the soluble boron concentration is ∓ 0.0006 Δk. No uncertainty has been reported for the buckling, but an arbitrary (and probably conservative) uncertainty of 10% was assumed. MCNP4C2 calculations for a change of ±10% in the axial bucking produce a corresponding change in reactivity of ∓0.0005 Δk. When combined, these two uncertainties produce an overall uncertainty of ±0.0008 Δk.

In addition to critical boron concentrations, measurements of fission rates at the core midplane were made in fuel pins in the central assembly of two of the benchmark configurations. Pin-by-pin relative fission rates for a symmetric octant of the central assembly are shown in Figures 4.1 and 4.2. Note that these relative fission rates were taken directly from Ref. 1 and that the average fission rate is not unity. The average fission rate to which all of the submitted results should be normalized is given in the figure captions.

The desired results for the core calculations include the effective multiplication factor (k_{eff}) and the pin-by-pin relative fission rates.

Water Hole	1.107 (0.2%)	1.026 (0.6%)	1.000 (0.1%)	1.025 (0.7%)	1.026 (0.3%)	0.980 (2.1%)	0.983 (0.8%)
	1.068 (0.2%)	1.075 (0.0%)	1.036 (0.7%)	1.047 (0.4%)	1.098 (0.6%)	1.026 (2.3%)	1.003 (3.1%)
		Water Hole	1.116 (1.1%)	1.118 (1.0%)	Water Hole	1.070 (0.9%)	0.961 (1.0%)
			1.091 (0.8%)	1.145 (0.7%)	1.133 (0.9%)	1.032 (2.5%)	0.924 (0.6%)
				Water Hole	1.109 (0.6%)	1.007 (1.4%)	0.974 (2.7%)
					1.015 (0.2%)	0.973 (2.4%)	0.974 (1.2%)
						0.970 (0.6%)	0.950 (0.5%)
							0.920 (1.4%)

Fig. 4.1 Measured pin-by-pin relative fission rates in symmetric octant of central assembly for core with assembly type B (loading 2). Values in parentheses are standard deviations obtained from two or more measurements (average fission rate is 1.0338).

Water Hole	1.148 (0.6%)	1.027 (0.4%)	1.045 (0.6%)	1.057 (0.6%)	1.047 (0.5%)	1.088 (0.4%)	1.124 (1.4%)
	1.036 (0.5%)	0.945 (0.7%)	1.001 (0.6%)	0.982 (2.1%)	0.962 (0.8%)	1.070 (1.3%)	1.105 (0.8%)
		Pyrex Rod	0.901 (0.7%)	0.900 (2.1%)	Pyrex Rod	1.001 (2.1%)	1.087 (0.6%)
			0.914 (0.4)	0.854 (2.0%)	0.933 (0.5%)	1.049 (1.3%)	1.088 (0.5%)
				Pyrex Rod	0.970 (1.2%)	1.097 (1.8%)	1.138 (1.3%)
					1.071 (0.6%)	1.140 (1.2%)	1.195 (0.5%)
						1.164 (0.3%)	1.199 (0.7%)
							1.206 (0.9%)

Fig. 4.2 Measured pin-by-pin relative fission rates in symmetric octant of central assembly for core with assembly type C (loading 8). Values in parentheses are standard deviations obtained from two or more measurements (average fission rate is 1.0416).

4.2 Lattice Calculations

There are a number of quantities which were not measured in the experiments but would prove useful in a comparison of different analysis techniques and basic data. Therefore, the following quantities for an infinite lattice should be computed:

- k_∞ = infinite-lattice multiplication factor
- normalized pin power distribution
- δ^{25} = ratio of epithermal-to-thermal fissions in ^{235}U
- δ^{28} = ratio of fissions in ^{238}U to fissions in ^{235}U
- ρ^{25} = ratio of epithermal-to-thermal captures in ^{235}U
- ρ^{28} = ratio of epithermal-to-thermal captures in ^{238}U
- CR = ^{238}U captures / ^{235}U absorptions
- Fraction of total absorptions in the Pyrex perturbing pins

The energy boundary to be used between thermal and epithermal is 0.625 eV.

4.3 Additional Information

A description of the methods and models employed is required for a useful comparison of methods. The following information, if appropriate, should be indicated:

- Isotopic number densities
- Cross section origin, library names and version (including any data modifications)
- Cross section processing codes (and version)
- Assembly calculation methodology (include code names and version)
- Core calculation methodology (include code names and version)
- Number of energy groups employed and energy group structure
- Any assumptions, approximations, or divergence from benchmark specifications

4.4 Format for Submission of Results

In order to facilitate the analysis and comparison of the participants' results, please submit the results in the format indicated in the Appendix. Submit hard copy and/or electronic file in a widely used format (MS Word, WordPerfect, or Adobe PDF).

5. REFERENCES

1. M. N. Baldwin and M. E. Stern, "Physics Verification Program, Part III, Task 4, Summary Report," Babcock & Wilcox report BAW-3647-20 (March 1971).

2. Russell D. Mosteller, "Critical Lattices of UO_2 Fuel Rods and Perturbing Rods in Borated Water," LEU-COMP-THERM-008, *International Handbook of Evaluated Criticality Safety Benchmark Experiments*, OECD Nuclear Energy Agency report NEA/NSC/DOC(95)03 (1996).

3. Theodore A. Parish, David J. Diamond, Russell D. Mosteller, and Jess C. Gehin, "Summary of Results for the Uranium Benchmark Problem of the ANS Ad Hoc Committee on Reactor Physics Benchmarks," pp. 1298-1305, *Proceedings of the International Conference on the Physics of Nuclear Science and Technology*, October 5-8, 1998, Long Island, New York, USA.

4. **Metals Handbook, Volume 2, 10th Edition**, ASM International (1990).

5. Robert C. Weast, Ed., **CRC Handbook of Chemistry and Physics, 58th Edition**, CRC Press, Inc. (1977).

6. Judith F. Briesmeister, Ed., "MCNP — A General Monte Carlo N-Particle Transport Code, Version 4C," Los Alamos National Laboratory report LA-13709-M (March 2000).

APPENDIX

PWR Lattice Benchmark Problems

Joint Benchmark Committee
of the
Mathematics and Computation, Radiation Shielding and Protection, and
Reactor Physics Divisions of the American Nuclear Society

Please submit results to:

Russell D. Mosteller
Los Alamos National Laboratory
MS F663
Los Alamos, NM 87545

Phone: (505) 665-4879
FAX: (505) 665-3046
e-mail: mosteller@lanl.gov

Name: _____

Organization: _____

Address: _____

_____

Phone: _____

FAX: _____

E-mail: _____

Please submit the results on the following forms or in a similar format. Include additional pages if necessary. Submission of partial results is acceptable if methodology or computer codes do not allow computation of complete results. Also submit the isotopic number densities used in the analysis in a convenient format.

Cross Sections Description:

Calculation Methodologies:

Core Calculation Results

Assembly type A effective multiplication factor:

Assembly type B effective multiplication factor:

Assembly type B pin-by-pin fission rates (include measured numbers and rms deviation)

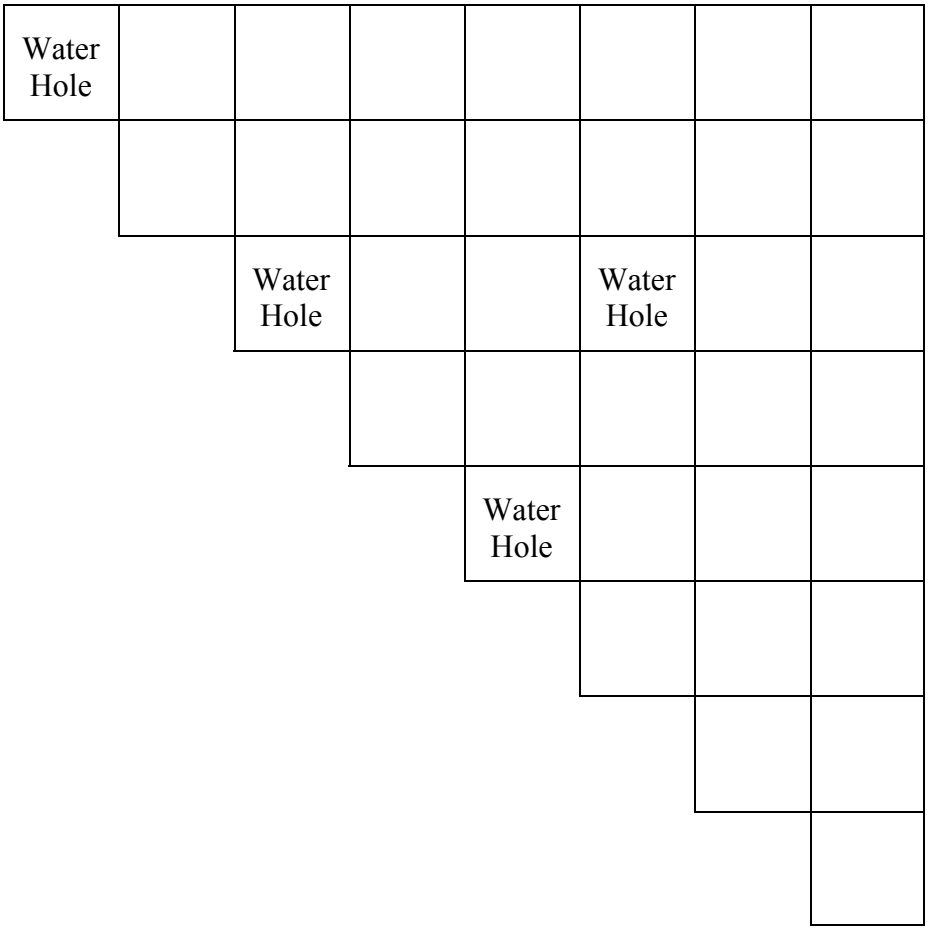

N. b.: Normalize to an average value of 1.0338.

Assembly type C effective multiplication factor:

Assembly type C pin-by-pin fission rates (include measured numbers and rms deviation)

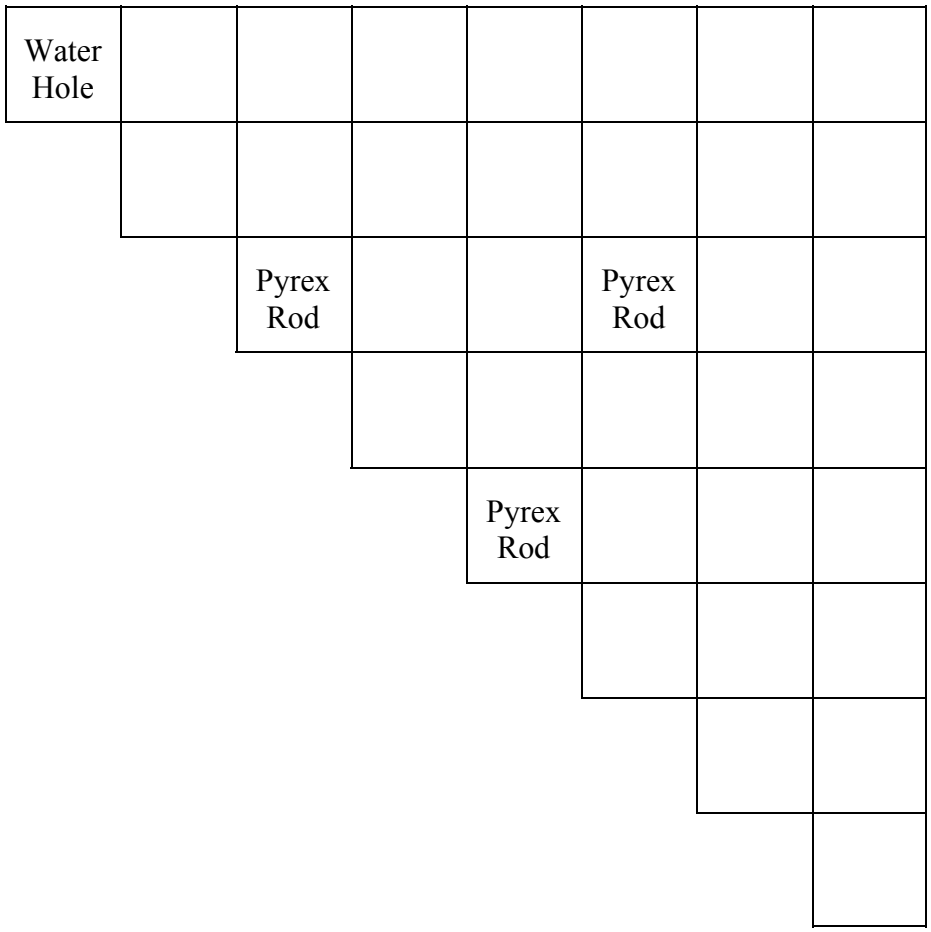

N. b.: Normalize to an average value of 1.0416.

Lattice Calculation Results

Assembly type A: infinite-medium multiplication factor:
δ^{25}:
δ^{28}:
ρ^{25}:
ρ^{28}:
CR:

Assembly type B: inifinite-medium multiplication factor:
δ^{25}:
δ^{28}:
ρ^{25}:
ρ^{28}:
CR:
pin-by-pin relative power distribution:

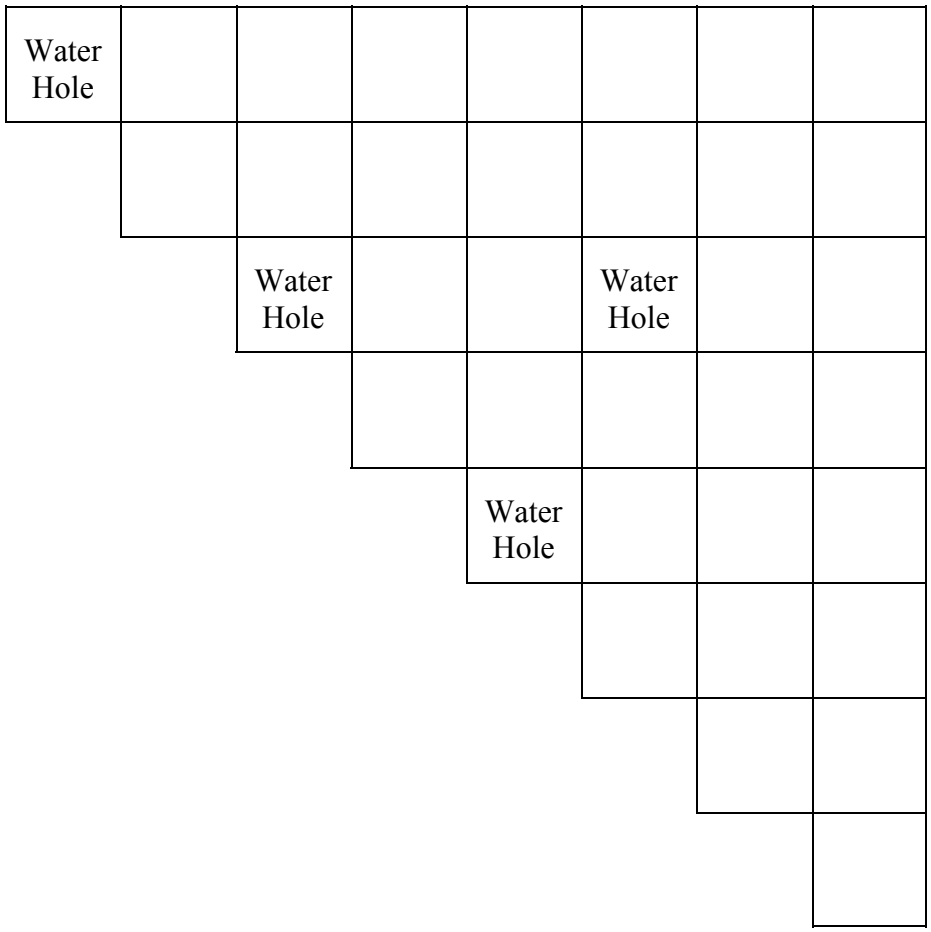

Assembly type C: infinite-medium multiplication factor:
δ^{25}:
δ^{28}:
ρ^{25}:
ρ^{28}:
CR:
Fractional absorption in Pyrex perturbing pins:
pin-by-pin relative power distribution: